

polymer papers

Coalescence and interfacial tension measurements for polymer melts: A technique using the spinning drop apparatus

G. E. Schoolenberg* and F. During

Shell International Chemicals B.V., Shell Research and Technology Centre,
 Amsterdam Badhuisweg 3, 1031 CM Amsterdam, The Netherlands

(Received 25 July 1995; revised 21 February 1997)

A novel technique that involves a spinning drop apparatus has been used to measure the interfacial tension of polymer melts on the basis of the shape of two colliding droplets. The technique combines the advantages of equilibrium techniques (accuracy and straightforward analysis) to a speed of measurement that is equal or faster than dynamic methods. For melt viscosity in the order of 10^4 Pas experimental time is in the order of 30 min. This is independent of viscosity ratio and interfacial tension itself, giving scope for investigating the effects of compatibilisers. Furthermore, the interfacial tension measurement is incorporated in a coalescence experiment. For the model systems chosen (PS/LDPE and PS/LLDPE) commercial polymers were shown to have reduced interfacial tension and increased scatter due to additives. When the polymers were purified the interfacial tension rose significantly. © 1997 Elsevier Science Ltd.

(Keywords: interfacial tension; spinning drop technique; coalescence)

INTRODUCTION

The mechanical properties of heterogeneous polymer blends strongly depend on the size of the dispersed particles (e.g. Refs. ^{1,2}). In blending the molten immiscible polymers by the application of a mixed elongational/shear flow-field, as in an extruder, droplets of the dispersed phase are gradually broken up into smaller ones (*Figure 1*).

Break-up will continue as long as the capillary number, Ca , is above a critical value, which is dependent on the viscosity ratio³. The capillary number is defined as:

$$Ca = \frac{\eta_m \dot{\gamma} R}{\sigma} \quad (1)$$

where η_m is the matrix viscosity, $\dot{\gamma}$ is the shear rate, R is the droplet radius and σ the interfacial tension.

Thus, it follows that the smaller the interfacial tension the smaller the minimum droplet size accessible through the break-up process. For large capillary numbers droplet break-up is a dominant phenomenon for polymer blends ($Ca > 1-10$, depending on the viscosity ratio).

At higher dispersed phase concentrations, the particles formed in the break-up process will frequently collide and coalescence of the droplets may occur (*Figure 2*). The size of the dispersed particles is then the result of the balance between break-up and coalescence behaviour in the applied flow-field.

To what extent coalescence will occur depends on the time of contact needed for two colliding droplets to actually coalesce. The rate-determining step in the coalescence process is usually the drainage of the matrix film separating the two droplets⁴. Coalescence time decreases with decreasing contact radius because of the shorter distance

over which the matrix has to be drained. Contact radii will decrease in size with decreasing droplet size and shear rate, and increasing interfacial tension. As a result, the regime where coalescence is dominant is characterised by small capillary numbers. Again the interfacial tension is an important parameter.

Apart from the contact radius, the coalescence time is also determined by the mobility of the interface and the rupture thickness of the matrix film separating the two droplets⁴. Depending on the value of these parameters, the capillary number below which coalescence will be dominant will be in the order of 0.1, so that in the region $0.1 < Ca < 10$ both processes (coalescence and break-up) take place simultaneously⁵⁻⁷.

Concluding, to predict the size of the dispersed phase resulting from a polymer blending process, the interfacial tension, interfacial mobility and rupture thickness should be known. Data on these parameters are in demand, but difficult to obtain experimentally. Experiments are laborious and prone to experimental error even for pure systems. Additional complications arise when compatibilisers are added or with commercial polymers which contain contaminations and additives causing scatter. In order to describe their effect one must be able to rapidly perform large series of measurements.

Here we describe a novel measuring technique which determines the three relevant parameters mentioned above, in a relatively fast experiment, using the spinning drop apparatus. The technique is demonstrated by measuring the specified parameters for a model system of a PS matrix with a PE dispersed phase. In this first report we will concentrate on the interfacial tension results. The results of coalescence experiments obtained with this model system will be discussed in a separate paper.

* To whom correspondence should be addressed



Figure 1 Droplet break-up in a shear flow

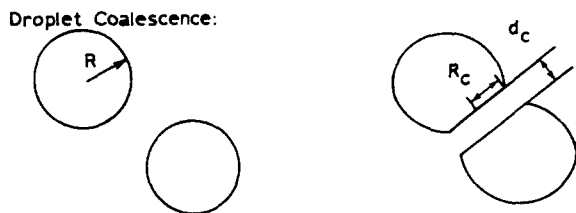


Figure 2 Droplet coalescence: R , droplet radius; R_c , contact (or matrix film) radius; d_c , matrix film thickness

LITERATURE

Interfacial tension measurements

Many traditional experiments to measure interfacial tension are based upon achieving gravity-induced droplet equilibrium shapes⁸⁻¹⁰. For polymers this is time consuming due to the highly viscous nature of the melt and the usually small density differences. A gravity-induced interfacial tension experiment such as the pendant drop method may take from several hours up to a number of days. During this time the polymers may suffer thermal degradation. A solution for this problem has been sought in working at lower temperatures, with low molecular weight analogues, combined with models to extrapolate the results to higher molecular weights and temperatures¹¹.

Dynamic methods to measure interfacial tension, such as the thread break-up^{12,13} and imbedded fibre retraction techniques¹⁴⁻¹⁹ can yield results relatively fast for moderate viscosities (say up to 10^2 Pa s). They rely on hydrodynamic interpretation of the (first stages of) spontaneous break-up or retraction of a fibre imbedded in a matrix. Therefore, these methods are quite sensitive to disturbances (orientation, internal stresses, shape irregularities) in the initial test specimens which influence the relaxation process. Samples need to be annealed carefully before use. Furthermore, the methods show complications when the material exhibits complex rheological features such as yield stresses^{12,13,15,16}.

Dynamic methods require zero shear viscosity data. For the retraction technique these have to be translated to an

effective viscosity which is not always straightforward especially for high viscosity ratios¹⁴. As viscosity increases to practical values (in the order of 10^4 Pas) even for these dynamic techniques the experiments become time consuming (with the risk of polymer degradation) and/or lose accuracy. In the case of the retracting fibre technique, Carriere and Cohen¹⁵ judge observation during 6 h necessary to obtain accurate results (within ca. 10%) for a system with 10^4 Pas viscosity. For the breaking thread technique experimental time can be reduced by reducing the thread diameter. However, diameters may have to be reduced to 10 micron or less, which will increase inaccuracy to well above 10%. Additionally for both techniques, but especially for the breaking thread method, increasing viscosity ratio $p = \eta_d/\eta_m$ more than proportionally increases experimental time. Also, time is increased proportionally with decreasing interfacial tension and increasing matrix viscosity.

Concluding, with these techniques the combination of accuracy and short experimental time is difficult to obtain. This will cause problems when practical systems are studied (e.g. Ref. 19), especially when compatibilisers are introduced which reduce interfacial tension and may increase viscosity and/or viscosity ratio. This is why an alternative technique is introduced using a spinning drop apparatus.

The spinning drop technique

In the past measuring interfacial tension from equilibrium droplet shapes has been successfully speeded up for polymers by using the spinning drop apparatus. It was first introduced by Vonnegut²⁰ and extended for use on polymer melts at higher temperatures e.g., by Patterson *et al.*²¹ and later by Elmendorp and de Vos²² and Elmendorp²³.

In the spinning drop apparatus (Figure 3) a droplet of one liquid is surrounded by a second, denser matrix liquid. The liquids are contained in a transparent cylinder which is rotated at a fixed speed. This introduces a centrifugal force field which drives the less dense liquid to the axis of the cylinder and the denser one to its perimeter. A cylinder of the lower density material with a concentric shell of the higher density material would arise, were it not for the counteracting effect of the interfacial tension of the two liquids. This minimises the interfacial energy and drives the droplet in the direction of the spherical shape it would obtain under quiescent conditions. After some time the droplet reaches an equilibrium shape under the action of the two opposing driving forces. For large droplets this shape can be approximated by a long cylinder with rounded ends. The interfacial tension can be calculated from the equilibrium shape.

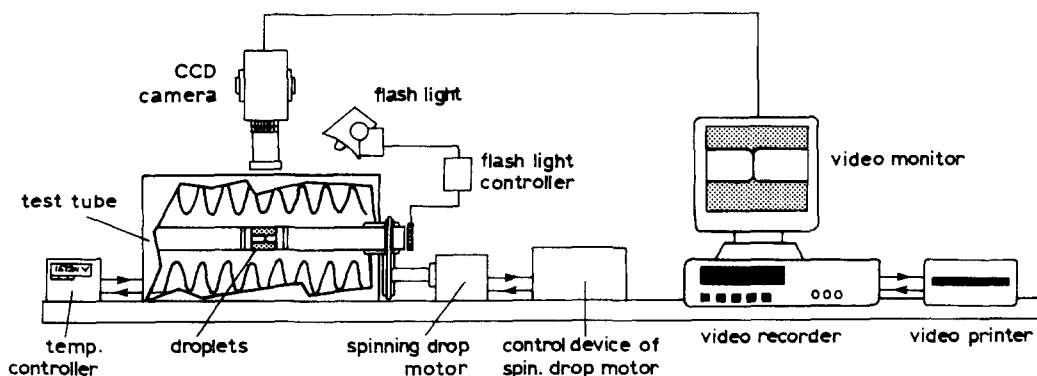


Figure 3 Spinning drop apparatus

Vonnegut²⁰ has given an equation which allows an approximation of the interfacial tension σ from the droplet radius of a large droplet in equilibrium conditions:

$$\sigma = \frac{\Delta\rho\omega^2 R_e^3}{4} \quad (2)$$

where $\Delta\rho$ is the density difference between the two phases, ω is the speed of rotation and R_e the equilibrium droplet radius.

Princen *et al.*²⁴ extended this method further with numerical solutions based on exact equations. However, for large droplets the equilibrium shape tends to be fairly elongated and therefore experiments in highly viscous polymer melts will still take much time (in the order of hours, depending on droplet size, viscosity and speed of rotation).

Elmendorp²⁵ has attempted to speed up the rate of measurement further by analytically describing the dynamics of the transformation from the initial spherical to the cylindrical equilibrium shape. More recently such a description was published based on numerical analysis by Hu and Joseph²⁶. In applying these methods some accuracy will be lost due to extrapolation to the final equilibrium shape and the experiment becomes quite laborious unless it can be monitored by image analysis equipment with the proper calculation procedures. The process still takes at least in the order of an hour.

So, though the spinning drop technique is generally accepted as a very accurate and relatively fast technique to measure interfacial tension (e.g. Refs. ^{13,22,23}), so far experimental time remained a disadvantage for high viscosities. However, by introducing a two-droplet method we have been able to reduce experimental time to *ca.* 10 minutes for low viscosity (10^2 Pas) systems up to 30 min for practical systems (10^4 Pas). This time is independent of interfacial tension and practically independent of viscosity ratio. Furthermore the procedure is an integrated part of a coalescence experiment between these droplets, which yields information on interfacial mobility and matrix film rupture thickness.

EXPERIMENTAL

Combined two-droplet experiment

Two droplets of dispersed phase material are inserted in the higher density matrix. Upon rotation they start to deform towards their equilibrium shape. Their size is chosen such that their joint equilibrium length during rotation is significantly larger than the available length in the experimental cylinder. Before reaching equilibrium shape, droplets will collide and start to exert a force upon one

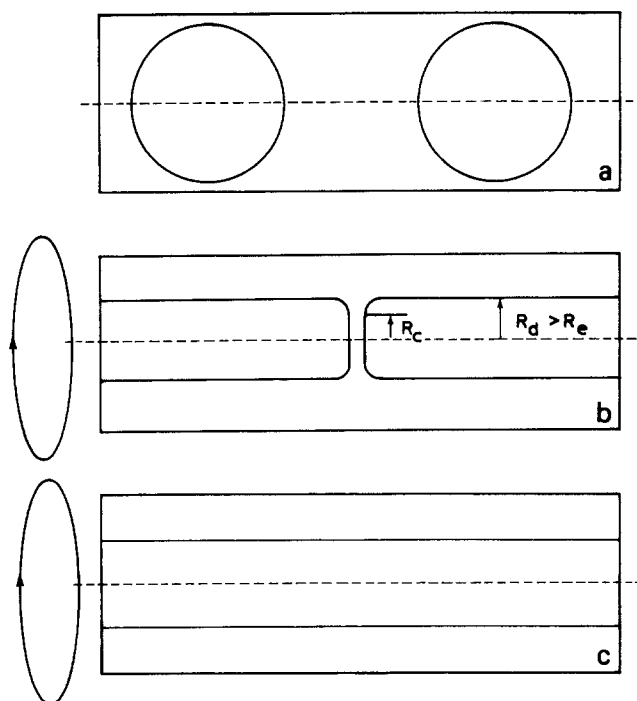


Figure 4 (a) Two droplets in the spinning drop chamber. (b) After deformation to the quasi-static situation (R_c contact radius, R_d outer radius). (c) After coalescence

another (Figure 4a). As a result their tips will flatten and a quasi-static situation sets in (Figure 4b). During this stage the shape of the droplets is constant while the matrix film between the two droplets thins. The thickness reduces from tenths of millimetres to, supposedly, a thickness in the order of nanometres (e.g. Ref. ⁴) at which the film ruptures and coalescence follows (Figure 4c). The time to reach the quasi-static situation, i.e. to measure interfacial tension, is typically 10–30 min for the systems experimented with (viscosities from *ca.* 10^2 to 10^4 Pas, viscosity ratio 0.03–300).

The experiment yields information on the interfacial tension through the shape of the droplets in the quasi-static situation. As will be shown here, this situation can be analytically described, with interfacial tension as the only unknown parameter. Thus, fitting the calculated shape to the one experimentally observed, by varying interfacial tension, allows us to measure the latter.

Spinning drop apparatus

The spinning drop apparatus used has been described elsewhere²¹. Its experimental chamber consists of a quartz cylinder which is rotated with a speed up to 2100 rad s^{-1} . The chamber can be heated up to 400°C . The quartz cylinder

Table 1 Characteristics of the materials

	η_0 at 220°C (Pa s)	M_n (kg mol ⁻¹) by GPC	M_w (kg mol ⁻¹) by GPC	M_w/M_n	M_z (kg mol ⁻¹) by GPC	M_z/M_w
PS1 (pure)	89	42	86	2.0	142	1.7
PS2	1300	77	184	2.4	341	1.9
PS2 (pure)	1000	77	184	2.4	341	1.9
PS3	9400	108	297	2.8	554	1.9
	η_0 at 220°C (Pa s)	M_n (kg mol ⁻¹) by GPC	M_w (kg mol ⁻¹) by GPC	M_w/M_n	M_w (kg mol ⁻¹) by light scatt.	No. of long branches/1000 C-atoms
LLDPE	307	15	52	3.5	80	–
LDPE 1	5600	17	94	5.5	282	1.9
LDPE 2	26000	19	108	5.7	325	1.2

is surrounded by thermal insulation except for a small window, where the droplets can be observed and video-taped through a microscope. A stable image is obtained by means of stroboscopic illumination.

The length of the cylinder is 150 mm and its internal diameter 5 mm. It contains a calibrating rod to determine the refractive index of the matrix at the measurement temperature. For the two-droplet experiment the chamber was additionally filled with glass rods to reduce its length to *ca.* 10 mm. Thus, the approach and flattening of the two droplets occur after a small deformation, thus shortening experimental time.

Materials

The feasibility of the two-droplet method is illustrated by results obtained with two PE/PS model systems on which ample reference data can be found in the literature. Materials used were low density polyethylene (LDPE), linear low density polyethylene (LLDPE) and polystyrene (PS) characterised by the data given in *Table 1*. PS1 was an extremely pure lab grade, whereas all other grades were commercially available. PS2 was used in its commercial variety and as the additive free precursor of this material (PS2 'pure') having the same molecular weight characteristics. The viscosity of PS2 'pure' is higher than for commercial PS2, since an internal lubricant to increase MFI is missing.

Density measurements were performed in a closed capillary rheometer (Instron MCR) loaded on an Instron TTD rig. Zero shear viscosity was measured on the same instrument using a cone and plate configuration. Note that since we describe an equilibrium method, viscosity is not a necessary parameter for the interfacial tension measurement, in contrast to dynamic methods. It is quoted here to allow comparison of the experimental time which increases strongly with viscosity for dynamic methods such as breaking thread and droplet retraction.

Sample preparation

Since PS is the denser phase it forms the matrix in the spinning drop experiment. Samples were prepared by compression moulding a 6-mm-thick plate of as received PS nibs in a vacuum mould at 200°C and 0.65 MPa. Rods of 10 mm length and 4.9 mm diameter were machined out of this plate. At the ends of this rod holes were drilled where the PE lumps, cut to obtain the desired droplet size, were inserted. The size or shape of the PE lumps is not critical, since they will be deformed to neat droplet shapes during melting and rotation. For convenience the two lumps were cut to approximately the same mass (i.e. same droplet size) which yields the quasi-static shape fastest. The cutting procedure takes no more than 5 min.

The commercial PE nibs were used as received. Furthermore, the LLDPE was used in a purified state. Purification took place by dissolving the polymer in toluene in an extraction column, filtering and then quenching the hot solution in methanol. All parts were cleaned in an ultrasonic bath with ethanol and dried in air. The glass cylinder, glass rods and calibration rod were cleaned in an oven at 500°C for 2 h.

Experimental procedure

After the cylinder has been filled, a vacuum is applied and the cylinder is placed in the pre-heated spinning drop apparatus. Once the polymer is molten, the calibrating rod is pressed into the cylinder to prevent air being sucked in.

After removal of the vacuum the cylinder is rotated at the desired speed and the experiment is recorded with a time lapse video. The experiments in this study took place at a temperature of 220°C and a speed of rotation of 2100 rad s⁻¹. *Figure 4* shows diagrams of the experiment in three stages of development: *a*, flattening droplets; *b*, quasi-static state; *c*, coalescence.

THEORETICAL RESULTS

Describing the quasi-static state: contact area and interfacial tension

For a single drop, Vonnegut²⁰ calculated the shape of the tips of the drop by assuming equilibrium at any cross section perpendicular to the droplet axis, between the forces in the direction parallel to the droplet axis. These forces originate from the interfacial tension (F_i) on the one hand and the pressure difference caused by the density difference in the centrifugal field (F_p) on the other. This can also be used here, but additionally we must deal with the coalescence force (F_c).

Clearly in the flattened contact area there is no component of the interfacial tension in the axial direction and we may state that:

$$F_c = F_p \text{ for } 0 < y < R_c \quad (3)$$

where R_c is the radius of the contact area.

On the other hand, beyond R_c there is no coalescent force and the forces due to the flow field generated by the film thinning process are expected to be negligibly small. Therefore we may state that:

$$F_i = F_p \text{ for } R_c < y < R_d \quad (4)$$

where R_d is the radius of the droplet on its cylindrical part. In the case of one single droplet the diameter of the cylindrical part of R_e (the radius of the droplet at equilibrium) is known from the thermodynamic equilibrium conditions. However, here R_d is determined by the inserted volume of the less dense fluid only. The pressure difference p_0 at the droplet's axis caused by the density difference and the centrifugal field is:

$$p_0 = \frac{\Delta\rho\omega^2 R_d^2}{2} + \frac{\sigma}{R_d} \quad (5)$$

And the pressure difference across any point of the droplet is:

$$p(y) = p_0 - \frac{\Delta\rho\omega^2 y^2}{2} = \frac{\Delta\rho\omega^2 (R_d^2 - y^2)}{2} + \frac{\sigma}{R_d} \quad (6)$$

The x component of the force caused by the pressure difference is obtained by integration

$$F_x = \int_0^{R_d} p(y) dA = \int_0^{R_d} p(y) 2\pi y dy \quad (7)$$

In the single droplet case further development of the equations is greatly simplified by the fact that from equation (2):

$$R_d = R_c = \left(\frac{4\sigma}{\omega^2 \Delta\rho} \right)^{1/3} \quad (8)$$

In the two-droplet case, the outer diameter R_d is determined by the volume of droplet material inserted. In the curved area the x component of the force which has to be balanced by the interfacial tension follows from integration of equation (6) over the area from R_c to the coordinate of

cross-section R :

$$F_x(y) = \int_{R_c}^R p(y) 2\pi y dy \quad (9)$$

Balancing this force with that due to the interfacial tension gives:

$$\begin{aligned} \pi \Delta \rho \omega^2 \left[\frac{R_d^2}{2} (R^2 - R_c^2) - \left(\frac{R^4}{4} - \frac{R_c^4}{4} \right) \right] + \pi \frac{\sigma}{R_d} (R^2 - R_c^2) \\ = 2\pi R \sigma \cos \theta \end{aligned} \quad (10)$$

where θ is the angle between the droplet axis and the interface.

At the cylindrical part of the droplet where $y = R_d$, equation (10) can be rewritten as:

$$\pi \Delta \rho \omega^2 \left[\left(\frac{R_d^2}{2} - \frac{R_c^2}{2} \right)^2 + \frac{R_c^3}{4} \left(R_d - \frac{R_c^2}{R_d} \right) \right] = 2\pi R_d \sigma \quad (11)$$

With equation (2) this leads to:

$$(R_d^2 - R_c^2)^2 - R_c^3 \left(R_d - \frac{R_c^2}{R_d} \right) = 2R_d R_c^3 \quad (12)$$

With $C = R_c/R_e$ and $D = R_d/R_e$ it follows that:

$$C = \sqrt{\frac{2D^3 + 1 - \sqrt{(8D^3 + 1)}}{2D}} \quad (13)$$

Since R_c and R_d can be measured, R_e and thus the interfacial tension can be calculated iteratively.

Shape of the droplet

Now that R_c is known, to describe the remainder of the profile equation (4), i.e. equation (10), should be valid at any coordinate y . Following Vonnegut we can rewrite:

$$\cos q = \frac{dx/dy}{\sqrt{1 + (dx/dy)^2}} \quad (14)$$

$$U = x/R_e \quad (15)$$

$$V = y/R_e \quad (16)$$

equation (10) can be rewritten as:

$$2D^2V^2 - 2D^2C^2 - V^4 + C^4 + \frac{V^2}{D} - \frac{C^2}{D} = 2V \frac{U'}{\sqrt{1 + U'^2}} \quad (17)$$

giving

$$U' = \frac{dU}{dV} = \frac{(V^2 - C^2)[2D^3 - D(V^2 + C^2) + 1]}{\sqrt{4V^2D^2 - (V^2 - C^2)^2[2D^3 - D(V^2 + C^2) + 1]^2}} \quad (18)$$

This allows us to calculate the droplet shape by a stepwise integration. A typical result for polymers is given in Figure 5.

EXPERIMENTAL RESULTS AND DISCUSSION

Accuracy of the measurement

Figure 6 shows an example of two droplets of PE in the quasi-static state. The method of operation is as follows: first the radius of the flattened contact area and the outer radius of the droplets are measured. Using equation

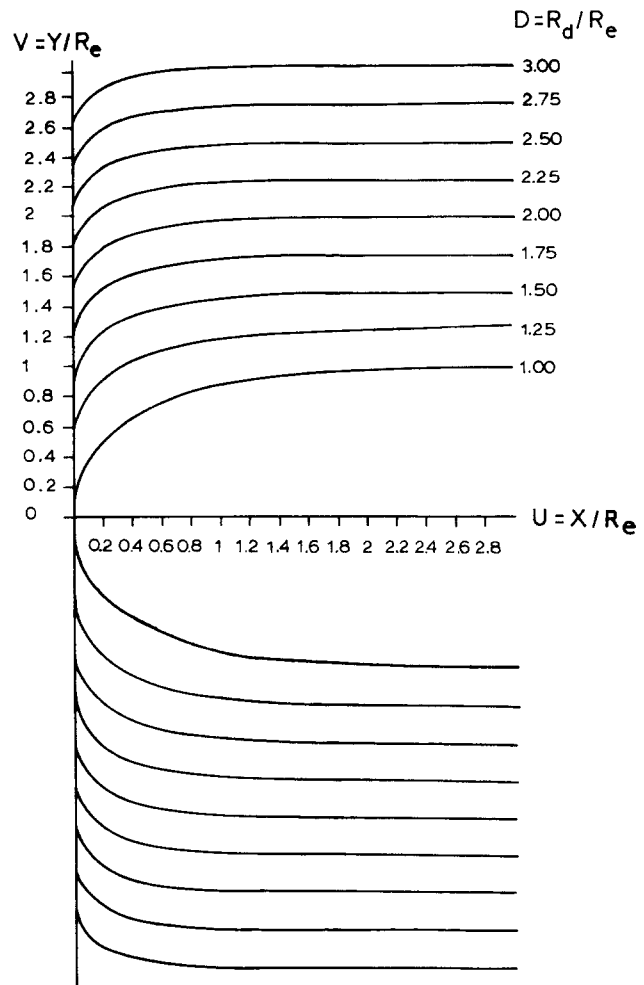


Figure 5 Typical results of droplet shapes with varying interfacial tension

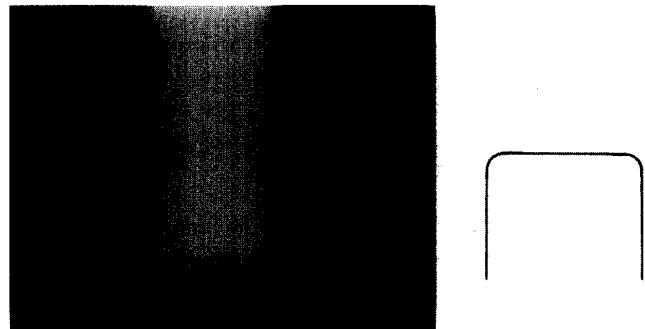


Figure 6 Example of curve fit to quasi-static droplet shape at 2100 rad s⁻¹ (20 000 rev min⁻¹)

(14), the relation with R_e , and the interfacial tension are determined.

Based on the accuracy with which the size measurements and the measurement of the density difference and rotation velocity can be performed, the interfacial tension value is accurate within 5–10% error, depending on the size of the droplet, the speed of rotation and the interfacial tension itself. Accuracy of the measurement mainly relies on the measurement of R . This is dependent on optical microscopic resolution. The best accuracy is obtained for large R_d and R_d/R_c ca. 0.5. Since the size of the droplets is rather large (compared with e.g. thread diameter in the breaking thread method) inaccuracy in measuring R is smaller, notably 1%.

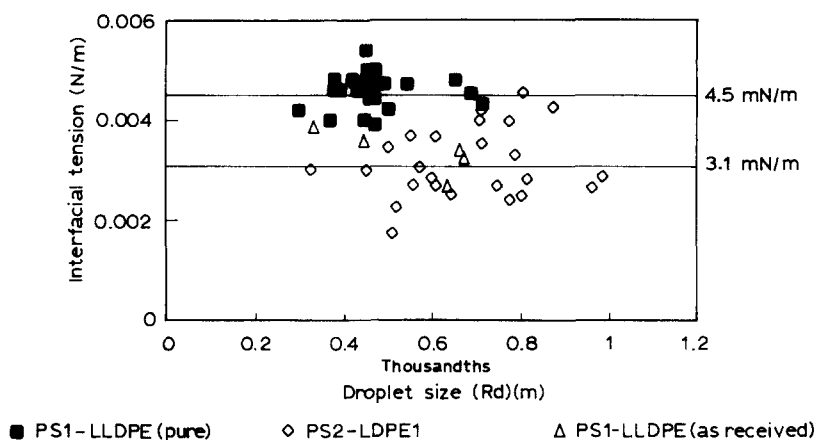


Figure 7 Interfacial tension versus droplet radius R_d

Errors in density difference are below 2.5% given the accuracy of the Instron equipment used. Rotation velocity can be measured with negligible inaccuracy. In similar conditions a single droplet experiment, fully deformed to its equilibrium shape will be slightly more accurate (within 3–7%), but this does not outweigh the much longer experimental time.

The method offers scope for further improved of the accuracy, by calculating the full shape of the droplet with equation (18) and adjusting the interfacial tension to obtain the best overall fit. This part of the procedure might in future be performed by using image analysis to determine the droplet shape. Our present equipment yielded insufficient contrast for fully automated image analysis. Because the accuracy obtained by manually measuring droplet radius was judged sufficient, we did not choose to improve on the hardware any further to achieve higher contrast. However, such improvements would be quite feasible.

Interfacial tension measurements at varying droplet size

Table 2 shows the results of all the combinations tested, while Figure 7 shows the range of measurements on the two systems most extensively tested with varying droplet size, which are printed in bold in Table 2.

Combination of the PS1 with the as received LLDPE gave an average interfacial tension of 3.3 mN m^{-1} (standard deviation 0.4 mN m^{-1} , i.e. 12% based on five measurements). This value is rather low compared with quotations in the literature, which are *ca.* 4.5 mN m^{-1} for PS/PE (e.g. Ref. 6,12,22). When the LLDPE was purified through a solvent route prior to use, as described in the experimental part, the average interfacial tension rose and the scatter of the data was reduced. The average value now lies in the expected range (4.5 mN m^{-1} , standard deviation 0.3 mN m^{-1} , i.e. 7%). Therefore, we assume that additives and impurities in the as received LLDPE are responsible for lowering the interfacial tension. That additives and impurities may have such effects is further confirmed by the results of the 'all-commercial' PS2-LDPE1 system, which yields an average value of 3.1 mN m^{-1} (standard deviation 0.7 mN m^{-1} , i.e. 22%). Similar values are obtained with LDPE 2. As mentioned above, in PS2 there is a small quantity of mineral oil to increase MFI, which probably reduces the interfacial tension with LDPE. Higher values are measured when LDPEs 1 and 2 are combined with the 'pure' PS1 and with PS3, and with the 'pure' PS2 grade which does not contain additives. Standard deviations are again in the order

Table 2 Interfacial tension at 220°C

	PS1 (pure)	PS2	PS2 (pure)	PS3
LLDPE	3.3	–	–	–
LLDPE (purified)	4.5	4.6	4.4	4.7
LDPE1	4.1	3.1	4.4	4.1
LDPE2	4.5	3.4	4.3	4.3

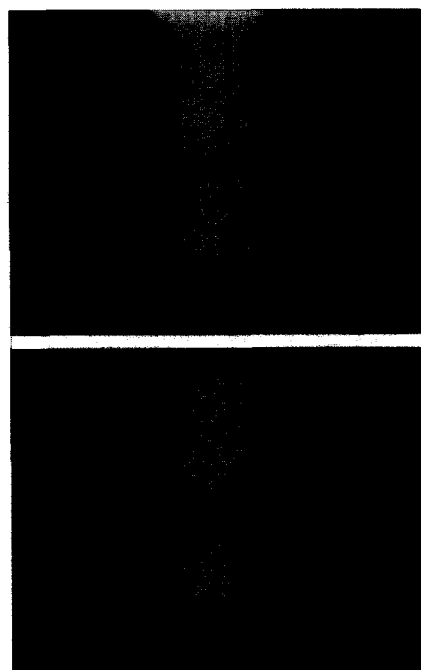


Figure 8 As for Fig. 6, tested at 1050 rad s^{-1} ($10000 \text{ rev min}^{-1}$)

of 7–10%. In the case of the purified LLDPE the effect of the mineral oil in PS2 could not be observed.

Interfacial tension measurement at varying speed of rotation to establish origin of scatter

From the various literature sources^{8,12–18,21} we conclude that the level of scatter encountered is usual. In fact a standard deviation in the order of 10–20% is considered quite acceptable^{12–18} by other authors. Based on the expected accuracy of the measurement, the scatter we observe is probably only partly due to experimental error. Apparently, as we will further demonstrate below, additives,

impurities and low molecular mass species present in the commercial grades not only reduce interfacial tension, but also cause sample to sample variations.

Figure 8 shows an example of the same commercial PS2/LDPE1 sample shown in Figure 6, here tested at half the rotation speed (1050 rad s^{-1}). Although the shape of the droplets is different, the calculation should yield the same value (in this sample 4.0 mN m^{-1}) for the interfacial tension, as indeed it does. We have performed this 'speed of rotation variation' using four speeds of rotation, for samples from the PS2/LDPE1 system. The standard deviation for various measurements for the same sample was 0.1 mN m^{-1} (2.5%) compared with 0.7 mN m^{-1} (22%) amongst various samples of this same system. That another measurement of the same sample, obtained by changing the speed of rotation, yields close to the same value of the interfacial tension, strengthens our opinion that the accuracy of the measurement is high in itself, and a large part of the above-mentioned scatter is due to true variation in the interfacial tension from sample to sample in the commercial systems. In some cases the relatively large scatter observed by other authors may be caused by similar effects.

CONCLUSIONS

It has been shown that the two-droplet spinning drop technique provides a measurement of interfacial tension combining the accuracy of equilibrium techniques to experimental times shorter or similar to those of dynamic techniques. The analysis involved is straightforward and relatively simple. The technique yields data which correspond well to data collected by other techniques to measure interfacial tension, but experimental time is shorter and experiments are feasible within 30 min for viscosities in the order of 10^4 Pas .

Furthermore, experimental time is independent of interfacial tension itself and viscosity ratio. This gives scope for measuring systems containing block-copolymer compatibilisers which increase viscosity and decrease interfacial tension. The first results of such measurements will be published in the near future²⁷.

Measurements on commercial and purified PS/PE systems show that additives, impurities and low molecular mass species reduce the interfacial tension. The technique developed allows testing the same sample under different conditions in rapid sequence. This shows that part of the large scatter in commercial systems is probably due to

inhomogeneous distribution of additives and impurities throughout samples.

REFERENCES

1. Bucknall, C. B., *Makromol. Chem., Makromol Symp.* (1988) 20/21 (Int. Symp. Mater. 1987) 425–439.
2. Borggreve, R. J. M., Gaymans, R. J., Schuijjer, J. and Ingen-Housz, J. F., *Polymer*, 1987, **28**(9), 1489.
3. Grace, H. P., *Chemical Engineering Communications*, 1982, **14**, 225.
4. Chesters, A. K., *Transactions of the Institute of Chemical Engineers, Part A*, 1991, **69**, 259.
5. Janssen, J. M. H., Dynamics of liquid-liquid mixing. Thesis University of Eindhoven, 1993.
6. Janssen, J. M. H., Peters, G. W. M., Meijer, H. E. H. and Baaijens, F. P. T., in *Theoretical and Applied Rheology. Proceedings of the 11th International Congress on Rheology*, Vol. 1. Elsevier, Amsterdam, 1992, pp. 369–371.
7. Janssen, J. M. H. and Meijer, H. E. H., *Journal of Rheology*, 1993, **37**(4), 597–608.
8. Wu, S., *Polymer Interface and Adhesion*. New York, 1982, pp. 257–274.
9. Anastasiadis, S. H., Chen, J. K., Koberstein, J. T., Sohn, J. E. and Emerson, J. A., *Polymer Engineering Science*, 1986, **26**(20), 1410.
10. Wagner, M. and Wolf, B. A., *Macromolecules*, 1993, **26**(24), 6498.
11. Mueller, M., *Kautschuk und Gummi, Kunststoffe*, 1993, **46**, 348.
12. Elemans, P. H. M., Modelling of the processing of incompatible polymer blends. Thesis, University of Eindhoven, 1989, Chapter 8.
13. Elemans, P. H. M., *Journal of Rheology*, 1991, **34**(8), 1322–1325.
14. Carriere, C. J., Cohen, A. and Arends, C. B., *Journal of Rheology*, 1989, **33**(5), 681–689.
15. Cohen, A. and Carriere, C. J., *Rheologica Acta*, 1989, **28**(3), 223.
16. Carriere, C. J. and Cohen, A., *Journal of Rheology*, 1991, **35**(2), 205–212.
17. Sammler, R. L., Dion, R. P., Carriere, C. J. and Cohen, A., *Rheologica Acta*, 1992, **31**(6), 554.
18. Ellington, P. C., Strand, D. A., Cohen, A., Sammler, R. L. and Carriere, C. J., *Macromolecules*, 1994, **27**, 1643–1647.
19. Lacroix, C., Bousima, M., Carreau, P. J., Favis, B. D. and Michel, A., *Polymer*, 1996, **37**(14), 2939–2947.
20. Vonnegut, B., *Review of Scientific Instruments*, 1942, **13**, 6.
21. Patterson, H. T., Hu, K. H. and Grindstaf, T. H., *Journal of Polymer Science (Part C)*, 1971, **34**, 31.
22. Elmendorp, J. J., A study on polymer blending microrheology. Thesis, University of Delft, 1986.
23. Elmendorp, J. J. and de Vos, G., *Polymer Engineering Science*, 1986, **26**(6), 415.
24. Princen, H. M., Zia, I. Y. and Mason, S. G., *Journal of Colloid and Interface Science*, 1967, **23**, 99.
25. Elmendorp, J. J., unpublished results.
26. Hu, H. H. and Joseph, D. D., *Journal of Colloid and Interface Science*, 1994, **162**, 331.
27. Schoolenberg, G. E. and During, F., accepted for Euromat conference, April 1997, Maastricht.